Ceramics International **21** (1994) 125–130

Observations of Delamination Fatigue on Pre-Cracked Ceramic Elements in Rolling Contact

M. Hadfield & T. A. Stolarski

Brunel University, Department of Mechanical Engineering, Uxbridge, Middlesex UB8 2PH, UK

(Received 8 March 1994; accepted 27 April 1994)

Abstract: Subsurface cracks on delaminated ceramic elements are experimentally investigated after testing in lubricated rolling contact conditions. In the case of hot isostatically pressed silicon nitride in contact with steel, radial and lateral pre-cracks initiate failure and the propagation mode is observed as delamination fatigue. The extent of subsurface crack length, depth and shape is investigated using a dye penetration method and an acoustic microscopy method. The observations of the subsurface crack provides evidence of lubricant driven delamination fatigue failure.

1 INTRODUCTION

The use of ceramic materials for elements in rolling contact bearings shows some practical advantages over traditional bearing steels. The properties of ceramics, specifically low density and high stiffness, are of most interest to gas-turbine,[1] and machine tool manufacturers.[2] Also high hardness, low coefficient of thermal expansion and high temperature capability are properties suited to rolling element bearing materials.

Research into the rolling contact fatigue performance of ceramics has intensified during the past decade. Technologies of powder manufacture and material densification have advanced to the stage that fully dense and high quality production of ceramics has become standardised.[3] Silicon nitride ceramic has been found to have the optimum combination of properties suitable for these applications. Research over the past two decades on its structure, quality control and manufacturing techniques has produced a material which can seriously be considered for rolling contact bearing design.[4] This is especially true for hybrid ball bearings, i.e. ceramic rolling elements and steel bearing races which are now available as standard industrial components. The modes of ceramic rolling contact fatigue failure, obtained from experimental tests have been studied.[5] The delamination failure mode of hot isostatically pressed silicon nitride and sintered sialon elements were investigated and classified in terms of initiation and propagation.[6] Pre-cracked hot pressed silicon nitride elements in contact with standard steel were also studied,[7,8] this revealed failure modes and identified subsurface failure stages.

In a previous study (Hadfield *et al.*[7]), experiments consisting of three artificially pre-cracked silicon nitride lower balls driven by a fourth contacting steel upper ball are described. This configuration models contact conditions within a hybrid rolling element ball bearing. Each ceramic lower ball is artificially damaged before testing by applying a number of indentations to each surface. In the case described radial cracks initiate a delamination fatigue failure mode on the ceramic surface. Subsurface cracks are investigated on the delamination and incipient failure regions. In this present study examination by optical, scanning electron and acoustic microscopy show some interesting insights into the failure mode, extent and shape of subsurface crack propagation.

Ceramics International. 0272-8842/95/$9.50

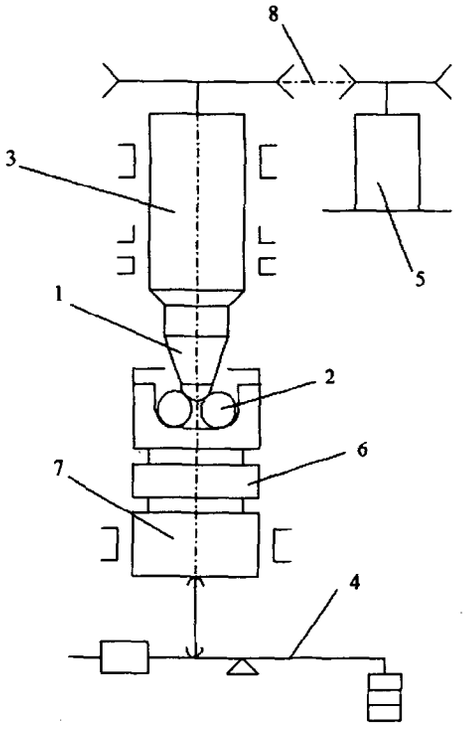

Fig. 1. Schematic representation of the modified four-ball machine: 1, upper-ball and collet; 2, lower-balls; 3, spindle; 4, loading lever; 5, driving motor; 6, heated plate; 7, loading piston; 8, belt drive.

2 EXPERIMENTAL PROCEDURE

2.1 Testing configuration

A modified four-ball machine shown as Fig. 1 is used to test pre-cracked ceramic elements. This modified machine is used as an accelerated method to compare the rolling contact fatigue resistance of materials under various tribological conditions. The machine consists of an assembly which models a rolling element ball bearing. The steel cup represents a bearing outer-race, three lower balls represent the balls within a bearing-race and an upper ball represents a bearing inner-race.

The assembly (Fig. 1) is loaded via a piston below the steel cup from a lever-arm load. The upper ball is assembled to a drive shaft via a collet, it contacts with three lower balls at a contact angle of 35·3°. Microslip occurs within the contact area due to deformation, this slip is typically between 3 and 5% and may be calculated by considering angular velocity at the contact centre. The contacting positions between the upper ball and lower balls are immersed with lubricating oil. A heater beneath the cup may be used to control lubricating oil bulk temperature. Spindle speed may be varied up to 20 000 rpm from high or low speed drives. Test time and spindle revolutions are recorded by a timer and tachometer. The machine may be set to stop either at revolution number or a maximum vibration amplitude. The machine has been used to examine rolling contact fatigue performance by various research staff. The Institute of Petroleum gathered various papers,[9] which describe various test results, ball dynamics and kinematics. Descriptions of lubrication effects and preliminary studies on ceramics,[10,11] have also been performed.

The material tested in this study is silicon nitride manufactured by the Hot Isostatically Pressed (HIP) route. Ball blanks are ground and polished to half inch diameter, standardised procedures are adopted to ensure consistent quality of material and geometry. Average roughness (R_a) of ceramic ball surface is 0·008 μm and ball roundness is within standard ball bearing tolerances. The steel upper ball which drives the ceramic test balls is grade 10 (ISO 3290-1975) carbon chromium steel with an average surface roughness of 0·020 μm and hardness of 64 HRC.

In this particular test described the rolling elements are lubricated with a high viscosity paraffin hydrocarbon lubricant which has a kinematic viscosity of 200 c.s.°C at 40°C and 40 c.s.°C at 100°C, this lubricant is not commercially available. The balls are loaded to a Hertzian contact pressure of 6·4 GPa, this is an extreme testing condition considering that rolling contact ball bearings operate at typically under half this contact value. Shaft/upper-ball speed is set at 5000 rpm. At these conditions the minimum film thickness may be calculated as 58 nm, although this figure is calculated using an estimated pressure–viscosity coefficient. The ratio of minimum film thickness to composite surface roughness is 2·5 which approximates to full film thickness at the contact plateau. It is understood that these elasto-hydrodynamic calculations must be treated with care for such critical film separations.

2.2 Pre-cracked silicon nitride balls

Each silicon nitride ball surface is artificially pre-cracked by nine equally spaced clusters of four indents. The indentations are produced by Vickers pyramid type heads with load set at 5 kg. This method produced indents, radial and lateral cracks on the ball surface. Radial pre-crack length was typically 0·1 mm and impression width 0·053 mm. Figure 2 shows a typical cluster of pre-cracks with spacing and typical crack dimensions. A dye penetrant method is employed to confirm the measurement of radial cracks and to identify subsurface lateral cracks. The localised stress field associated with these indents and cracks is described by Ueda.[12]

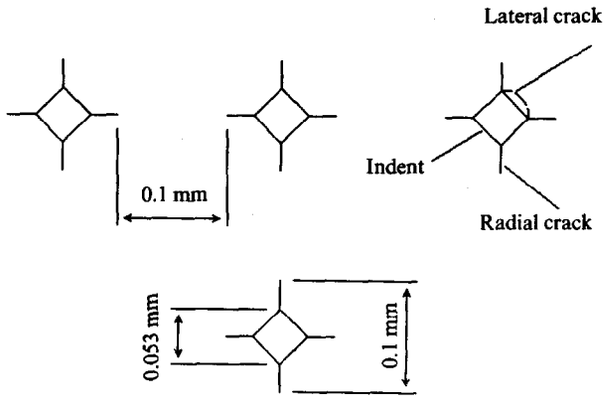

Fig. 2. Indents and pre-cracks on ceramic ball surface.

2.3 Test results

This test was terminated by the vibration cut-out device after 14.0 million load cycles had been applied to the steel upper ball. Results and discussion of how the lubricant influences time to failure and failure mode is illustrated from additional tests on pre-cracked ceramic elements as given by Hadfield.[7,8] The final bulk temperature of the lubricant stabilised at 75°C due to elastic deformation hysteresis[13] from ambient 25°C which is typical for a test under these conditions and duration. It is difficult to ascertain the exact lower ball fatigue cycles on such a small area of the surface. The kinematics of the lower balls is complex[14] due to the velocities in the orbit and spin planes and therefore it is not practical for positioning to a particular contact path.

It was evident from the initial observation[7] that the upper-steel ball had failed by a delaminated surface spall fatigue mode. The steel upper ball contact path did not show any evidence of permanent deformation, edge cracks or secondary pitting. Test vibration amplitude increase and hence termination was due to this steel upper ball fatigue failure.

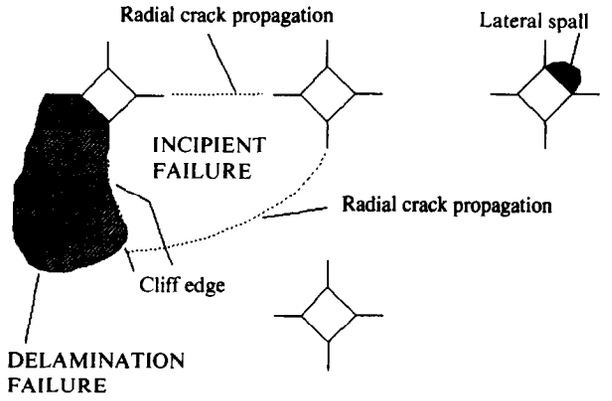

Fig. 3. Indents and pre-cracks after test.

After an initial microscopic observation of each ceramic lower ball, evidence of delamination fatigue failure, incipient delamination failure, radial crack growth and lateral crack spalling was found (Fig. 3). The incipient failed area is bounded by radial crack growth and a delamination failure. It should be stated that these surface failures were non-catastrophic, sustainable and did not cause abrasive wear on any of the contacting surfaces. The following surface analysis is performed on this particularly interesting delamination and incipient delamination failure.

3 SURFACE ANALYSIS OF CERAMIC FAILURE

Scanning electron microscope overview observations of the ceramic delamination and incipient delamination are shown in Fig. 4. The complete failed area, Fig. 4(a), shows the extent of radial crack growth which connects two indentations with the delaminated area. The failed area of approximately 0·065 mm^2 is composed of a delaminated and an incipient failure of similar size. The delaminated area shows a typical morphology observed previously in surface studies on perfect ceramic

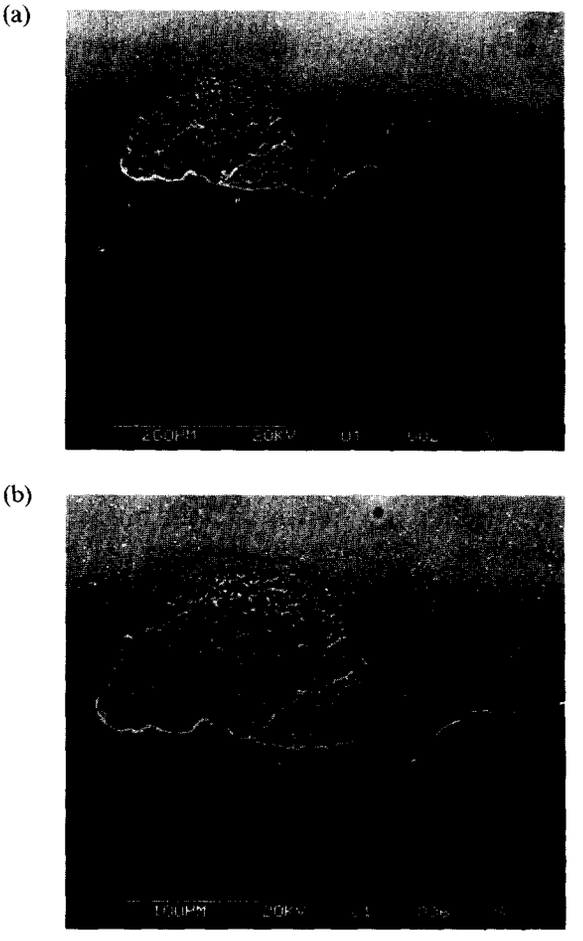

Fig. 4. Scanning electron microscope observations: (a) failed area; (b) delamination failure.

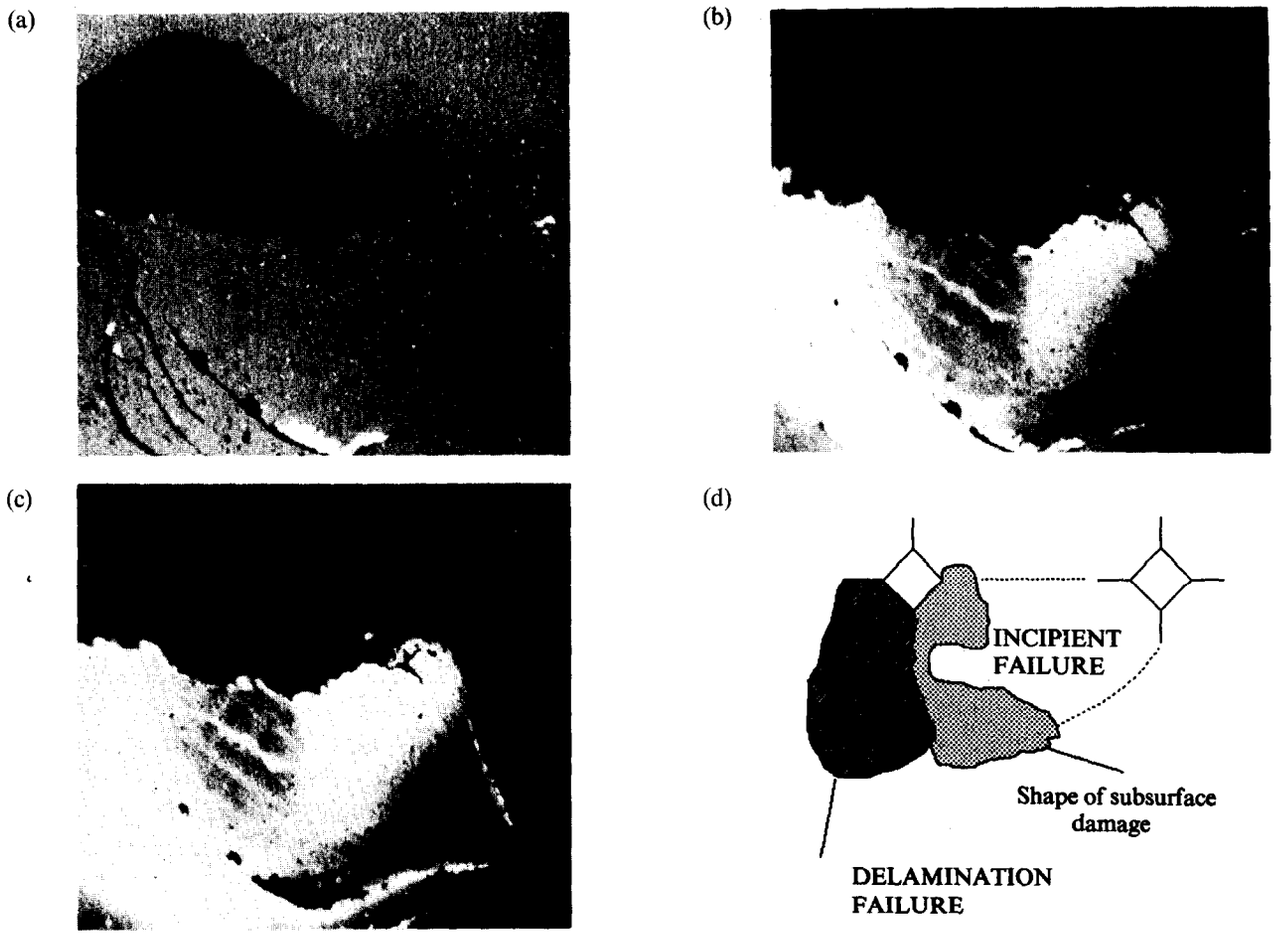

Fig. 5. Light microscopic observations: (a) white light (×170); (b) mixed light (×170); (c) ultraviolet light (×170); (d) schematic diagram.

test elements.[5,6] The adjacent incipient delamination fatigue failure is large compared with other experimental test results.[14] Commencement of the subsurface crack is positioned at the failure cliff base and is shown in Fig. 4(b), the delamination maximum depth is 30 μm from the stylus profile.

At this stage the extent of the subsurface crack beneath the intact surface is unknown and therefore experimental methods of observing this are adopted. The first method is a dye penetration technique, results are shown as light microscopic images in Fig. 5. During this method the ball is chemically cleaned and treated with a dye penetrant and a chemical removal process. The general failed area, Fig. 5(a), under white light shows the characteristic of the damage, again radial crack propagation is clear and the dark area is the delaminated surface. At this stage the incipient delamination is implied by the surrounding radial crack propagation adjacent to the failed area. The same view, Fig. 5(b), is shown under mixed white and ultraviolet light. In this case the extent of the subsurface separation beneath the incipient surface is evident. Fluorescent dye which has penetrated beneath the surface is visible due to the translucency of the silicon nitride material. Under ultraviolet light only, Fig. 5(c) shows the extent of the subsurface damage more clearly, radial crack propagation is also more visible. It can be seen that the extent of the subsurface crack is significant and penetration extends approximately 70 μm from the delamination cliff. The schematic diagram, Fig. 5(d), shows the general shape and extent of the subsurface damage in relation to the delamination area and propagated radial cracks.

A scanning acoustic microscope is employed to quantify incipient delaminated subsurface crack depth and confirm the extent of damage observed using the dye penetration method. This technique is especially useful for subsurface crack observations of ceramics which are traditionally difficult to experimentally analyze as explained in Ref. 15. Images produced from reflected acoustic waves are shown in Fig. 6. In this case the scan width is at 0·5 mm and acoustic wave frequency is set at 200 MHz. A surface image, Fig. 6(a), corresponds to the lower indentation of the ceramic failure, showing the two radial crack propagation and the incipient delamination surface. Figure 6(b) shows the subsurface image at the same position at a

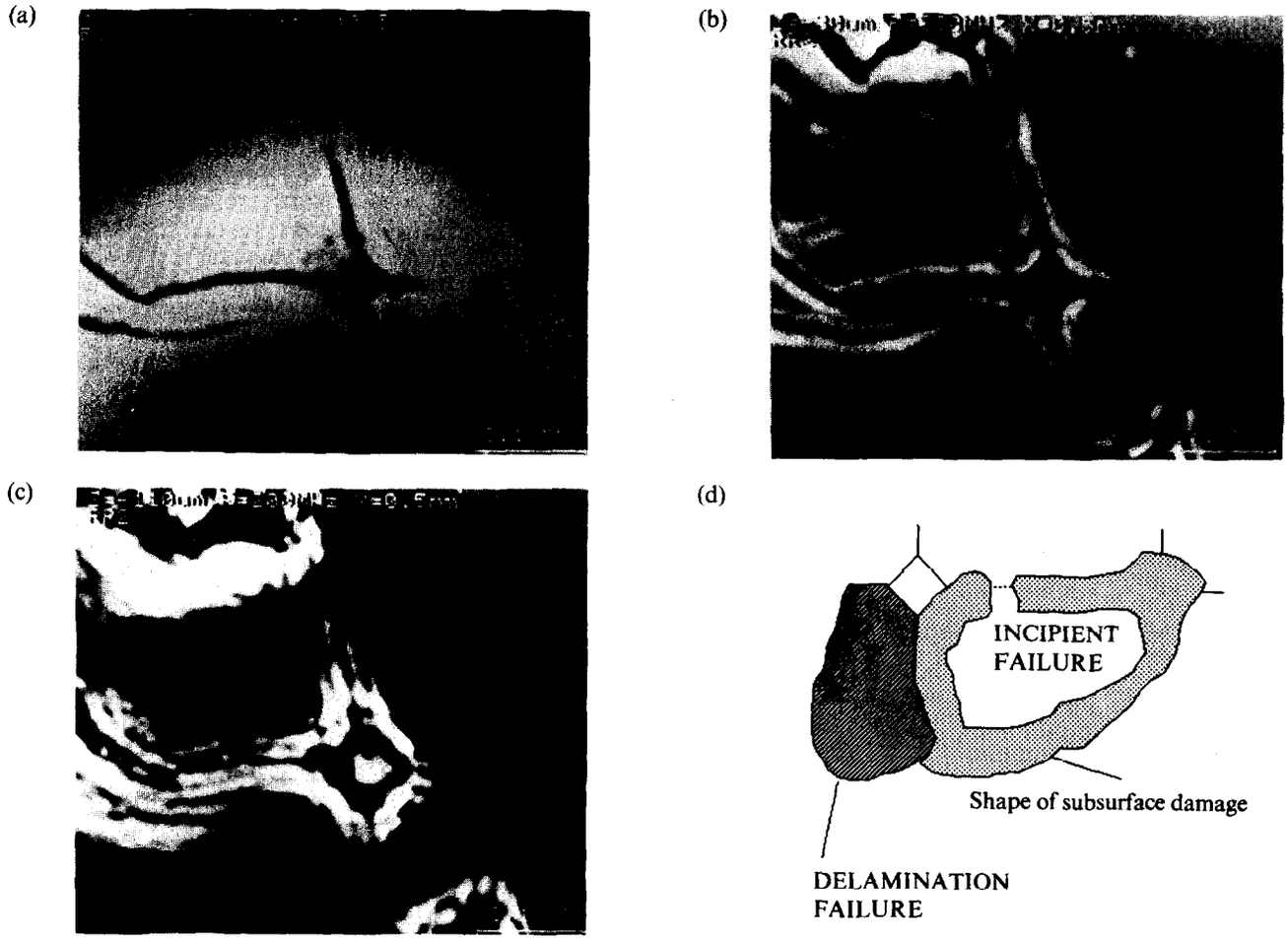

Fig. 6. Scanning acoustic image: (a) surface image; (b) at 3·75 μm depth; (c) at 13·75 μm depth; (d) schematic diagram at 13·75 μm.

depth of 3·75 μm below the surface. In this case the area of the incipient delamination is reduced which illustrates the extent of shallow subsurface cracks located close to the failure boundary. The next image, Fig. 6(c), is located at a position of 13·75 μm below the surface. At this depth the subsurface cracks are evident from the white areas and have propagated 100 μm from the delamination cliff and 35 μm from the radial cracks. This subsurface damage reduces the intact incipient area to 0·18 mm^2. A schematic diagram Fig. 6(d), shows the general shape of the subsurface damaged area at the maximum measured depth of 13·75 μm.

This result has confirmed the earlier examinations that subsurface crack damage may propagate relatively large distances from the surface damage. This points towards the hypothesis that the crack opening and closing mechanism is caused by hydrostatic lubricant pressure which is capable of driving surface cracks to eventual delamination failure. The delamination theory of sliding wear proposed by Suh[16,17] reports compelling similarities to the results described. It is appreciated that the friction coefficients during modified four-ball testing are very small compared with the original delamination theory.

4 CONCLUDING REMARKS

Results from dye penetration and acoustic microscopy studies on pre-cracked silicon nitride balls tested in rolling contact provide some evidence that the lubricant plays an important role in delamination fatigue failure.

It is believed that the lubricant enters the opened crack and it is trapped there when the crack is closed. As a result a substantial hydrostatic lubricant pressure is developed which is capable of propagating the crack to eventual delamination failure.

REFERENCES

1. HAMBURG, G., COWLEY, P. & VALORI, R., *Operation of an All-Ceramic Mainshaft Roller Bearing in a J-402 Gas-Turbine Engine*, ed. J. Asle. Lubrication Engineering, July 1980.
2. ARAMAKI, H., SHODA, Y., MORISHITA, T. & SAWAMOTO, T., The performance of ball bearings with silicon nitride ceramic balls in high speed spindles for machine tools. *J. Tribol.*, **110** (1988) 693–8.

3. CUNDILL, R. T., High precision silicon nitride balls for bearings. *SPIE*, Vol. 1573 Commercial Applications of Precision Manufacturing at the Sub-Micron Level (1991).
4. NISHIHARA, Y., NAKASHIMA, H., TSUSHIMA, N. & ITO, S., Factors that affect rolling contact fatigue life of ceramics and rolling contact fatigue life of ceramic balls and rollers. *ASME*, 90-GT-377.
5. HADFIELD, M., STOLARSKI, T. A. & CUNDILL, R. T., Failure modes of ceramics in rolling contact. *Roy. Soc. Proc. Ser. A*, **443** (1993) 607–21.
6. HADFIELD, M., STOLARSKI, T. A. & CUNDILL, R. T., Delamination of ceramic balls in rolling contact. *Ceramics Int.*, **19**(3) (1993) 151–8.
7. HADFIELD, M., STOLARSKI, T. A., CUNDILL, R. T. & HORTON, S., Failure modes of pre-cracked ceramic elements under rolling contact. *Wear*, **169** (1993) 69–75.
8. HADFIELD, M., STOLARSKI, T. A., CUNDILL, R. T. HORTON, S., Failure modes of ceramic elements with ring-crack defects. *Tribol. Int.*, **26**(3) (1993) 157–64.
9. TOURRET, R. & WRIGHT, E. P., Rolling contact fatigue: performance testing of lubricants. *Int. Symp., I. Petroleum*, October 1976. Heyden & Son Ltd, London (1977).
10. SCOTT, D. & BLACKWELL, J., Hot pressed silicon nitride as a rolling bearing material — a preliminary assessment. *Wear*, **24** (1973) 61–7.
11. SCOTT, D., BLACKWELL, J. & MCCULLAGH, P. J., Silicon nitride as a rolling bearing material — a preliminary assessment. *Wear*, **17** (1971) 73–82.
12. UEDA, K., Contact-stress deformation and fracture in ceramics. *Jap. J. Tribol.*, **34** (1989) 123–31.
13. TABOR, D., The mechanism of rolling friction. *Roy. Soc. Proc. Ser. A*, **229** (1955) 198–220.
14. HADFIELD. M., Rolling contact fatigue of ceramics, PhD Thesis, Brunel University, Published by the British Library, March 1993.
15. HADFIELD, M., STOLARSKI, T. A. & TOBE, S., Subsurface crack investigation on delaminated ceramic elements. *Tribol. Int.*, **27** (1994) 359–67.
16. SUH, N. P., The delamination theory of wear. *Wear*, **25** (1973) 111–24.
17. SUH, N. P., *Tribophysics*. Prentice-Hall, 1986.